J|A|C|S
ARTICLES
Published on Web 03/27/2002

Photoinduced Electron-Transfer Processes along Molecular Wires Based on Phenylenevinylene Oligomers: A Quantum-Chemical Insight

G. Pourtois,[†,‡] D. Beljonne,[†,‡] J. Cornil,[†,‡] M. A. Ratner,[§] and J. L. Brédas*[,†,‡]

Contribution from the Laboratory for Chemistry of Novel Materials, University of Mons-Hainaut, 20, Place du Parc, B-7000 Mons, Belgium, Department of Chemistry, The University of Arizona, Tucson, Arizona 85721, and Department of Chemistry and Materials Research Center, Northwestern University, 2145 North Sheridan Road, Evanston, Illinois 60208

Received September 24, 2001

Abstract: Quantum-chemical techniques are applied to model the mechanisms of photoinduced charge transfer from a π-electron donating group (tetracene, D) to a π-electron-acceptor moiety (pyromellitimide, A) separated by a bridge of increasing size (*p*-phenylenevinylene oligomers, B). Correlated Hartree−Fock semiempirical approaches are exploited to calculate the four main parameters controlling the transfer rate (k_{RP}) in the framework of Marcus−Jortner−Levich's formalism: (i) the electronic coupling between the initial and final states; (ii) and (iii) the internal and external reorganization energy terms; and (iv) the variation of the free Gibbs energy. The charge transfer is shown to proceed in these compounds through two competing mechanisms, coherent (superexchange) versus incoherent (bridge-mediated) pathways. While superexchange is the dominant mechanism for short bridges, incoherent transfer through hopping along the phenylene vinylene segment takes over in longer chains (for ca. three phenylenevinylene repeat units). The influence of the chemical structure of the π-conjugated phenylenevinylene bridge on the electronic properties and the rate of charge transfer is also investigated.

I. Introduction

Electron-transfer reactions between chemical species or subunits of a single compound play a key role in many biological[1−4] processes and in materials science.[5,6] The understanding and control of these reactions have long been the subject of intense research activity. The stakes are not only fundamental but also have strong implications for the development of numerous applications in optoelectronics such as solar cells.[6−10] In recent years, many studies have been devoted to the characterization of the mechanisms of long-range charge-transfer processes taking place from a π-electron donating group to an electron acceptor moiety through a molecular "bridge"[11−15] in donor−bridge−acceptor (DBA) assemblies.[11−15]

Theoretical investigations, based on a variety of quantum-chemical techniques, have provided insight into the possible pathways for charge-transfer processes and have highlighted the crucial role played by the electronic coupling between the donor and the acceptor, which primarily governs the distance dependence of the electron-transfer rates.[16,17] It is generally accepted that two limiting cases can be used to describe electron-transfer reactions. When the donor and the acceptor are weakly coupled with the bridge, the transfer takes place directly from the donor to the acceptor via a tunneling process (also referred to as superexchange mechanism) and exhibits an exponential decay as a function of the distance, *d*, between the donor and the acceptor:

$$k_{RP} \approx \exp(-\beta d) \qquad (1)$$

β typically varies from 0.2 [18−20] to 1.4 Å^{-1} [21,22] depending on the systems under consideration.

* To whom correspondence should be addressed. E-mail: jlbredas@u.arizona.edu.
† University of Mons-Hainaut.
‡ The University of Arizona.
§ Northwestern University.

(1) Jortner, J. *J. Chem. Phys.* **1976**, *64*, 4860.
(2) De Vault, D.; Chance, B. *Biophys. J.* **1966**, *6*, 825.
(3) Armitage, B. *Chem. Rev.* **1998**, *98*, 1171.
(4) Schuster, G. B. *Acc. Chem. Res.* **2000**, *33*, 253.
(5) Zerza, G.; Sharber, M. C.; Brabec, C. J.; Sariciftci, N. S.; Gómez, R.; Segura, J. L.; Martin, N.; Srdanov, V. I. *J. Phys. Chem. A* **2000**, *104*, 8315.
(6) Dittmer, J. J.; Marseglia, E. A.; Friend, R. H. *Adv. Mater.* **2000**, *12*, 1270.
(7) Sariftci, N. S.; Smilowitz, L.; Heeger, A. J. *Science* **1992**, *258*, 1474.
(8) Yu, G.; Gao, J.; Hummelen, J. C.; Wudl, F.; Heeger, A. J. *Science* **1995**, *270*, 1789.
(9) Brabec, C. J.; Padinger, F.; Hummelen, J. C.; Sariftci, N. S. *Appl. Phys. Lett.* **1999**, *85*, 6866.
(10) Nitzan, A. *Annu. Rev. Phys. Chem.* **2001**, *52*, 681.
(11) Nishitani, S.; Kurate, N.; Sukata, Y.; Misumi, S.; Karen, A. *J. Am. Chem. Soc.* **1983**, *105*, 1983.
(12) Joran, A. D.; Leland, B. A.; Geller, G. G.; Hopfield, J. J.; Dervan, P. B. *J. Am. Chem. Soc.* **1984**, *106*, 6090.
(13) Pfinckh, P.; Heitele, H.; Volk, M.; Michel-Beyerle, M. E. *J. Phys. Chem.* **1988**, *92*, 6584.
(14) Wiederrecht, G. P.; Niemczyk, M. P.; Svec, W. A.; Wasielewski, M. R. *J. Am. Chem. Soc.* **1996**, *118*, 81.
(15) Creager, S.; Yu, C. J.; Bamdad, C.; O'Connor, S.; MacLean, T.; Lam, E.; Chong, Y.; Olsen, G. T.; Luo, J.; Gozin, M.; Kayyem, J. F. *J. Am. Chem. Soc.* **1999**, *121*, 1059.
(16) Naleway, C. A.; Curtiss, L. A.; Miller, J. R. *J. Phys. Chem.* **1991**, *95*, 8434.
(17) Newton, M. D. In *Advances in Chemical Physics*; Jortner, J., Bixon, M., Eds.; John Wiley and Sons: New York, 1999; Vol. 1, pp 303−375.
(18) Kelley, S. O.; Barton, J. K. *Science* **1999**, *283*, 375.
(19) Tolbert, L. M. *Acc. Chem. Res.* **1992**, *25*, 561.

10.1021/ja017150+ CCC: $22.00

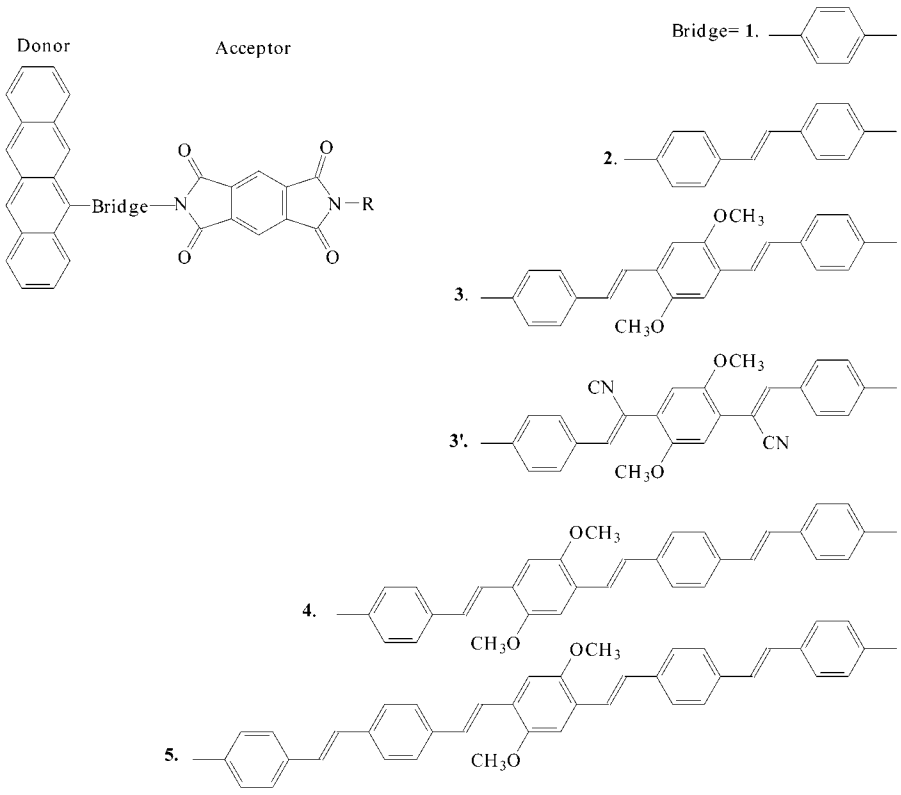

Figure 1. Chemical structures of the molecules investigated.

For larger effective couplings, the transfer can be mediated by the "bridge", this being, for instance, a protein,[22] a DNA segment,[18] or a conjugated oligomeric backbone.[13,20] There, in the incoherent regime, the photoinduced electron-transfer proceeds in two steps: the charge is first transferred from the excited donor (D*) to the conjugated bridge, leading to the formation of an intermediate D^+B^- species; electron transfer from the bridge to the acceptor then occurs to complete the global charge-transfer process. Another possible bridge-mediated mechanism allowing for long-range charge-transfer processes (weak distance dependence of the transfer rates) relies on the formation of superdonor and/or superacceptor units in the initial or final state, which results from a delocalization over the bridge of the donor or acceptor levels involved in the process; in this coherent regime,[23] the transfer occurs by a direct transfer (as is the case for superexchange) without giving rise to the appearance of intermediate charge-transfer species.

Recently, Davis et al.[24] have synthesized molecules in which a donor (tetracene) and an acceptor (pyromellitimide) are anchored at the extremities of *p*-phenylene vinylene segments of increasing size; see Figure 1. Upon selective photoexcitation of the donor unit, they have observed using time-resolved spectroscopy that electron transfer occurs from the donor to the acceptor and leads to a quenching of the tetracene emission. They have suggested from their results that the mechanism leading to charge-transfer varies with the length of the conjugated bridge. The main goal of our work is to provide, on the basis of correlated calculations, quantitative estimates of the electronic and thermodynamic parameters determining the relative efficiency of the superexchange and coherent versus incoherent bridge-mediated mechanisms in these DBA compounds.

The paper is organized as follows. We first describe the theoretical methodology used to evaluate the charge-transfer rates. We then focus on the chain-length dependence of the electronic and optical properties of the DBA molecules and determine the set of molecular parameters required to estimate the charge-transfer rate for the various mechanisms from Marcus−Jortner−Levich's expression.[25−27] We finally compare the calculated electron-transfer rates to the corresponding experimental data and assess the nature of the possible mechanisms.

II. Theoretical Methodology

In all cases, the electron-transfer process is initiated through photoexcitation of the donor by a vertical electronic transition from the ground state (hereafter denoted as DBA) in its equilibrium geometry (Q_G) to the excited-state D*BA, followed by a nuclear relaxation on the excited-state potential energy curve toward the equilibrium geometry Q_R; see Figure 2. The dissociation of the electron−hole pair via a charge-transfer process from the relaxed D*BA (Q_R) state to the charge-separated state D^+BA^- (Q_P) can then take place (it is usually assumed that geometric relaxation in the initial D*BA state proceeds faster than electron transfer).

(20) Arrhenius, T. S.; Blanchard-Desce, M.; Dvolaitzky, M.; Lehn, J. M.; Malthete, J. *Proc. Natl. Acad. Sci. U.S.A.* **1986**, *83*, 5355.
(21) Winkler, J. R.; Gray, H. B. *Chem. Rev.* **1992**, *92*, 369.
(22) Moser, C. C.; Kseske, J. M.; Warncke, K.; Farid, R. S.; Dutton, P. L. *Nature* **1992**, *355*, 796.
(23) Bixon, M.; Jortner, J. In *Advances in Chemical Physics*; Jortner, J., Bixon, M., Eds.; John Wiley and Sons: New York, 1999; Vol. 1, pp 35−202.
(24) Davis, W. B.; Svec, W. A.; Ratner, M. A.; Wasielewski, M. R. *Nature* **1998**, *396*, 60.
(25) Ulstrup, J.; Bixon, M. *J. Chem. Phys.* **1975**, *63*, 4358.
(26) Efrima, S.; Bixon, M. *Chem. Phys. Lett.* **1974**, *25*, 34.
(27) Efrima, S.; Bixon, M. *Chem. Phys.* **1976**, *13*, 447.

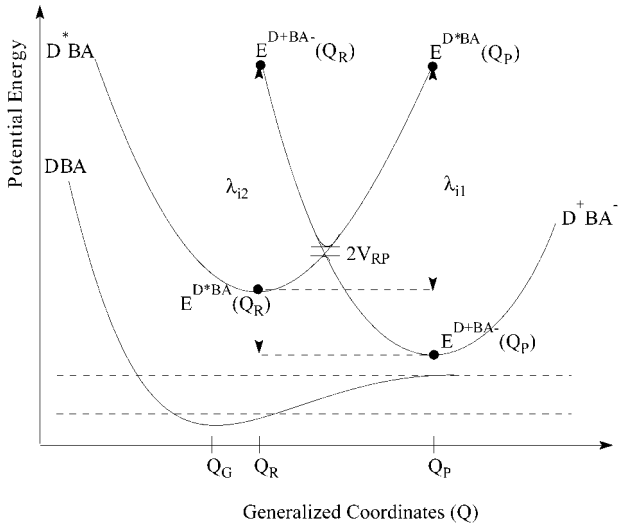

Figure 2. Schematic representation of the excited-state potential energy curves involved in the photoinduced charge-transfer process with respect to the generalized coordinates of the ground, excited, and charge-transfer states (Q_G, Q_R, and Q_P). The λ_{i1} and λ_{i2} terms describe the internal relaxation energies when the charge separation (going from Q_R to Q_P) and the recombination processes (going from Q_P to Q_R) are considered, respectively. The generalized coordinate is dominated by C−C bond distortions, as is expected for π-conjugated compounds.

In the weak coupling limit (electronic coupling smaller than reorganization energy or thermal energy spacing), the rate of photoinduced charge transfer, k_{RP}, between an initial state associated to the reactant, R, and a final state corresponding to the product, P, is given by the Fermi golden rule for radiationless transitions (in this paper, R and P can vary; R is D*BA or D^+B^-A, while P is D^+B^-A or D^+BA^-):

$$k_{RP} = \frac{2\pi}{\hbar} V_{RP}^2 (\mathrm{FCWD}) \tag{2}$$

V_{RP} is the electronic coupling term between the diabatic electronic wave functions of the initial and final states, Ψ_R and Ψ_P:

$$V_{RP} = \langle \Psi_R | H | \Psi_P \rangle \tag{3}$$

FCWD is the Franck−Condon weighted density of states taking into account the density of vibrational levels in both the initial and the final states and their Franck−Condon overlap. According to Marcus theory, the Franck−Condon overlap should incorporate the vibrational modes of the molecule (ω_i) and those of the surrounding medium (ω_s).[27]

To a first approximation, the vibrational modes (ω_i) of the molecule can be treated quantum mechanically (i.e., by assuming that $\hbar\omega_i \gg kT$) with the introduction of a single effective mode of frequency $\langle\omega\rangle$ representative of the dominant modes assisting the transfer in the molecular system;[28,29] in contrast, a classical description can be taken for the solvent vibrational modes (ω_s), since usually $h\omega_s \ll kT$. In such instances, the FCWD term can be rewritten as

$$\mathrm{FCWD} = \left(\frac{1}{4\pi\lambda_s kT}\right)^{1/2} \sum_v e^{-S} \frac{S^v}{v!} \exp\left(-\frac{(\Delta G^0 + \lambda_s + v\hbar\langle\omega\rangle)^2}{4\lambda_s kT}\right) \tag{4}$$

where λ_s describes the reorganization energy of the solvent as induced by the electron transfer, $\Delta G°$ is the variation of the free Gibbs energy during the reaction, and S is the Huang−Rhys factor; the latter is expressed in terms of the inner reorganization energy λ_i and the effective mode vibrational energy $\hbar\langle\omega_i\rangle$:

$$S = \frac{\lambda_i}{\hbar\langle\omega_i\rangle} \tag{5}$$

The inner reorganization energy (λ_i) corresponds to the energy required to accommodate the nuclear rearrangements occurring upon charge transfer when going from the equilibrium geometry of the photoexcited state (Q_R) to that of the charge-transfer state (Q_P). When the two parabolas representing the two states have a different curvature, λ_i is typically estimated as the average[30] value of the λ_{i1} and λ_{i2} terms depicted in Figure 2:

$$\lambda_i = \frac{\lambda_{i1} + \lambda_{i2}}{2} \tag{6}$$

Because the molecules under study can be effectively described as three individual units (mainly as a consequence of large torsion angles between donor, bridge, and acceptor, vide infra), λ_{i1} and λ_{i2} can be defined to a very good approximation as

$$\lambda_{i1} = E^{D^*BA}(Q_P) - E^{D^*BA}(Q_R) \approx (E^{D^*}(Q_P) + E^{A}(Q_P)) - (E^{D^*}(Q_R) + E^{A}(Q_R)) \tag{7}$$

$$\lambda_{i2} = E^{D+BA^-}(Q_R) - E^{D+BA^-}(Q_P) \approx (E^{D^+}(Q_R) + E^{A^-}(Q_R)) - (E^{D^+}(Q_P) + E^{A^-}(Q_P)) \tag{8}$$

where E^{D^*}, E^{D+}, E^{A}, and E^{A-} refer to the total energy of the isolated donor in its lowest singlet-excited state and cationic state and that of the isolated acceptor in the ground state and anionic state, respectively. Equations 7 and 8 define the overall λ_I for the D*BA → D^+BA^- transition. Their applicability is confirmed by the results of the actual calculations, which show localization on D* in the photoexcited reactant and on D^+ and A^- in the product. As indicated in ref 31, this localization is indeed facilitated by large torsion angles.

Here, the ground-state geometry of the DBA molecules and their separate moieties has been optimized by means of the semiempirical Hartree−Fock austin model 1[32] (AM1) method, which is known to provide reliable ground-state geometric structures for conjugated organic molecules.[33−35] The excited and/or ionized equilibrium geometries of the isolated units have been obtained by combining the AM1 approach to a complete active space configuration interaction (AM1/CAS-CI) treatment (as developed in the AMPAC package[36]); the excited-state geometries of the whole supramolecule are then built from the adequate relaxed geometries of the isolated chromophores. The

(28) Sutin, N. In *Advances in Chemical Physics*; Jortner, J., Bixon, M., Eds.; John Wiley and Sons: New York, 1999; Vol. 1, pp 7−34.
(29) Vanduyne, R. P.; Fischer, S. F. *Chem. Phys.* **1974**, *5*, 183.
(30) Marcus, R. A. *J. Chem. Phys.* **1965**, *43*, 679.
(31) Davis, W. B.; Ratner, M. A.; Wasielewski, M. *J. Am. Chem. Soc.* **2001**, *123*, 7877.
(32) Dewar, M. J. S.; Zoebisch, E. G.; Healy, E. F.; Stewart, J. J. P. *J. Am. Chem. Soc.* **1995**, *117*, 3702.
(33) Cornil, J.; Beljonne, D.; Brédas, J. L. *J. Chem. Phys.* **1995**, *103*, 843.
(34) Almlöf, J.; Fischer, T. H.; Gassman, P. G.; Ghosh, A.; Häser, M. *J. Phys. Chem.* **1993**, *97*, 10964.
(35) Merchan, M.; Orti, E.; Roos, B. O. *Chem. Phys. Lett.* **1994**, *226*, 27.
(36) *Ampac*, 6.55 ed.; Semichem: Shawnee, KS, 1997.

size of the active space in the AM1/CAS-CI calculations has been modulated to ensure convergence of the total energy and geometric parameters. The number of occupied and unoccupied molecular orbitals involved in the active space typically varies from 5 to 20 along the series of studied bridges. Note that the AM1/CAS-CI procedure used here was found to properly account for the lattice relaxation phenomena occurring in the neutral excited state[37,38] and charged ground state[39] of phenylene-based conjugated molecules.

The solvent reorganization energy (λ_s) can be estimated from the classical dielectric continuum model developed by Marcus.[30] This model assumes that the time scale of the electron-transfer process is much faster than that associated to the solvent nuclear reorganization. Accordingly, the electron transfer across the DBA molecule induces an electronic polarization of the medium that stabilizes the charge-transfer state. In his initial work, Marcus used spherical cavities surrounding the ionized donor and acceptor units to model the stabilization of the charge-separated state by the solvent; the latter was calculated for spherical cavities of radii R_D for the donor and R_A for the acceptor knowing the center-to-center distance (l_{DA}) and the optical and static dielectric constant of the medium, ϵ_{op} and ϵ_s, respectively. Although this formalism is justified for charge transfer between spherical species, such as for ion exchange reactions, it does not appear to be appropriate for the quasi one-dimensional conjugated units under study. We have thus adopted ellipsoidal cavities (of fitted dimensions R_x, R_y, R_z) for the two building units of the DBA molecules taking part in the electron-transfer process (eq 9). The reorganization energy is then expressed as

$$\lambda_s = \frac{(\Delta q)^2}{2}\left(\frac{1}{\sqrt[3]{(R_X R_Y R_Z)_D}} + \frac{1}{\sqrt[3]{(R_X R_Y R_Z)_A}} - \frac{2}{l_{DA}}\right)\left(\frac{1}{\epsilon_{op}} - \frac{1}{\epsilon_s}\right) \tag{9}$$

where Δq is the amount of charge transferred between the donor and the acceptor.

The static and optical dielectric constants of 2-methyltetrahydrofuran (1.98 and 6.97, respectively), one of the solvents used in the experimental studies of Davis et al.,[24] have been chosen to allow for a direct comparison between the experimental and calculated transfer rates.

Experimentally, $\Delta G°$ is evaluated on the basis of the Weller equation[40] that involves the constituents active in the transfer process. For a photoinduced electron transfer from a donor to an acceptor in a DBA molecule, $\Delta G°$ is estimated from the difference between the oxidation ($E_{D+/D}$) and reduction ($E_{A-/A}$) potentials of the redox species, from which the excitation energy of the donor (E^*) and the Coulomb stabilization of the D^+A^- pair (separated by a distance r_{AD}) in solution are subtracted:

$$\Delta G° = E_{(D+/D)} - E_{(A/A-)} - E^* - E_{Cb} \tag{10}$$

$$E_{Cb} = \frac{1}{4\pi\epsilon_0}\frac{e^2}{\epsilon_s r_{AD}} \tag{11}$$

In a similar way, we compute $\Delta G°$, for instance, for the transition between the D*BA and D^+BA^- states from the free energy variations associated to the oxidation of the donor in the excited state ($\Delta G°_{(D+/D^*)}$) and the reduction of the acceptor $\Delta G°_{(A-/A)}$ in the ground state and by further subtracting the Coulomb term E_{Cb}:

$$\Delta G° = \Delta G°_{(D+/D^*)} - \Delta G°_{(A-/A)} - E_{Cb} \tag{12}$$

We neglect here the change in entropy induced by the electron transfer, which is expected to be generally much smaller than the enthalpy variation. In our approach, $\Delta G°$ is thus evaluated on the basis of enthalpies of formation (ΔH_f^0) as

$$\Delta G°_{(D+/D^*)} - \Delta G°_{(A/A-)} \approx (\Delta H^0_{f,(D+)} + \Delta H^0_{f,(A-)}) - (\Delta H^0_{f,(D^*)} + \Delta H^0_{f,(A)}) \tag{13}$$

The heats of formation have been computed at the AM1/CAS-CI level, the influence of the solvent being taken into account by means of the COSMO software[41] implemented in the AMPAC package. The Coulomb stabilization E_{Cb} has been determined by summing the paired interactions between the partial atomic charges q_i and q_j separated by a distance r_{ij}, as calculated at the AM1/COSMO level for the ionized donor D^+ and acceptor A^-, respectively.

$$E_{Cb} = \frac{1}{4\pi\epsilon_0}\sum_{i}^{\text{acceptor}}\sum_{j}^{\text{donor}}\frac{q_i q_j}{\epsilon_s r_{ij}} \tag{14}$$

The electronic coupling (V_{RP}) between the initial and final states is evaluated in the Fermi golden rule formalism on the basis of a diabatic description of the excited-state wave functions. This cannot be readily applied to our correlated quantum-chemical calculations, which explicitly take into account the D−A interactions and hence provide an adiabatic description of the system. However, use of the generalized Mulliken−Hush formalism (GMH) recently developed by Cave and Newton[42] allows us to evaluate V_{RP} for a photoinduced charge transfer from quantities derived from an adiabatic description:

$$V_{RP} = \frac{\mu_{RP}\Delta E_{RP}}{\sqrt{(\Delta\mu_{RP})^2 + 4(\mu_{RP})^2}} \tag{15}$$

This expression involves the energy difference (ΔE_{RP}), as well as the corresponding dipole moment difference ($\Delta\mu_{RP}$) and transition dipole moment (μ_{RP}), between the initial and final states. We have computed these parameters in the nuclear arrangement representative of the initial state (Q_R)[43] (and without taking into account the solvent effects) by means of the semiempirical Hartree−Fock INDO (intermediate neglect of differential overlap[44]) Hamiltonian coupled to a configuration

(37) Beljonne, D.; Shuai, Z.; Friend, R. H.; Brédas, J. L. *J. Chem. Phys.* **1995**, *102*, 2042.
(38) Cornil, J.; Beljonne, D.; Heller, C. M.; Campbell, I. H.; Laurich, B. K.; Smith, D. L.; Brédas, J. L. *Chem. Phys. Lett.* **1997**, *278*, 139.
(39) Beljonne, D.; Cornil, J.; Sirringhaus, H.; Brown, P. J.; Shkunov, M.; Friend, R. H.; Brédas, J. L. *Adv. Funct. Mater.* **2001**, *11*, 229.
(40) Rhem, D.; Weller, A. *Isr. J. Chem.* **1970**, *8*, 59.
(41) Klamt, A.; Schürmann, G. *J. Chem. Soc., Perkin Trans.* **1993**, *2*, 799.
(42) Cave, J. C.; Newton, M. D. *Chem. Phys. Lett.* **1996**, *249*, 15.
(43) Within the Condon approximation, the electronic coupling is assumed to be independent from the nuclear coordinates. This approximation, which holds in most cases, breaks down, however, for large distortions in the equilibrium geometry when going from reactants to products; such a breakdown has, for instance, been demonstrated in a substituted biphenyl derivative for large inter-ring torsion angles, see: Toutounji, M. M.; Ratner, M. A. *J. Phys. Chem. A* **2000**, *104*, 8566.
(44) Ridley, J.; Zerner, M. C. *Theor. Chim. Acta* **1973**, *32*, 111.

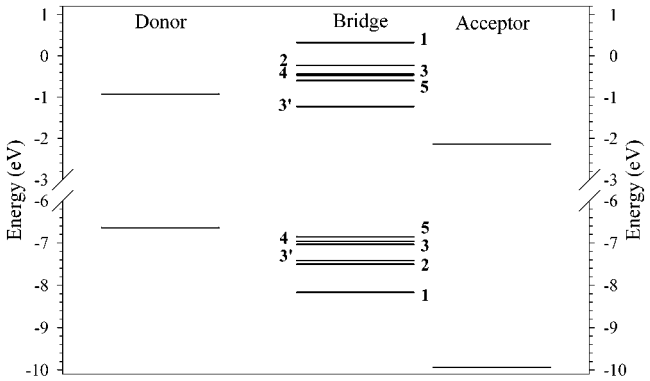

Figure 3. Schematic energy diagram showing the highest occupied (bottom part) and lowest unoccupied (top part) molecular orbitals, as computed at the INDO level for the subunits constituting **1**, **2**, **3**, **3′**, **4**, and **5**.

interaction scheme involving single excitations (SCI) with respect to the Hartree−Fock determinant (the Mataga−Nishimoto[45] potential is used to describe the electron−electron interactions). The size of the active space is increased until complete convergence of the transition energies from the ground state to the lowest excited states is achieved (the number of electronic configurations evolves from 900 for molecule **1** to 4000 for molecule **5**).

Note that the energies of the excited states are typically overestimated at the AM1 level by about 1 eV with respect to INDO. We give more confidence to the results provided by the INDO/S Hamiltonian, which has been specifically parametrized to reproduce the optical absorption spectra of organic molecules when coupled to a SCI scheme. It is worth pointing out that the semiempirical technique used here to compute the electronic couplings has been validated for a number of model redox systems; see, for instance, ref 46. Comparison between V_{RP} values based on INDO and ab initio results was found to provide agreement within 20%. Note also that we carried out test calculations on the shortest compounds using more elaborate treatments such as the coupled cluster single and double (CCSD) approach[47] and found no appreciable changes in the description of the excited states with respect to the SCI results.

III. Results and Discussion

A. Electronic Structure and Optical Properties. As a result of donor−bridge and bridge−acceptor steric interactions, the molecular wires adopt a nonplanar conformation characterized by torsion angles between the donor and the bridge and between the bridge and the acceptor of 72° and 30°, respectively. These twist angles induce localization of the molecular orbitals on the different moieties of the DBA molecule, which therefore keep most of their individual electronic properties.

The progressive increase in the conjugation length of the bridge when going from **1** to **5** gives rise to a gradual decrease in its HOMO−LUMO gap. The relative efficiency of the superexchange versus bridge-mediated mechanisms can be gauged *qualitatively* by examining the one-electron structure of the different compounds; see Figure 3 (although a correlated treatment is necessary to provide quantitative values of the transition energies to the excited states involved in the charge-transfer process, vide infra). In **1** and **2**, the energy of the LUMO

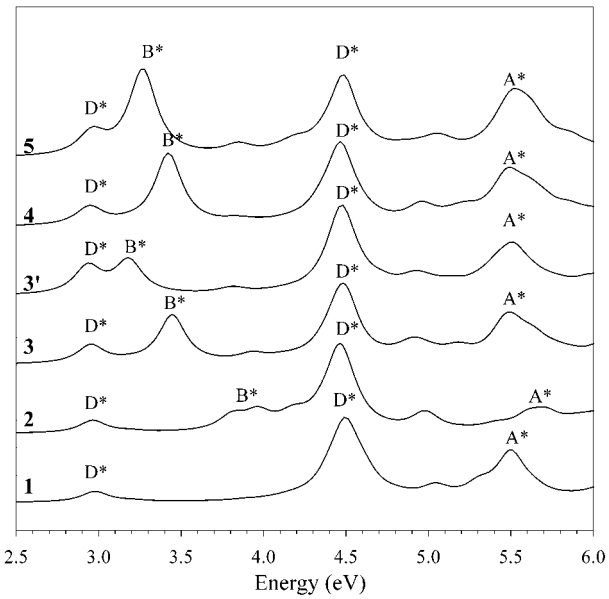

Figure 4. INDO/SCI simulated absorption spectra of the DBA compounds.

level of the bridge is much higher than that of the donor (by 1.4 and 0.9 eV for **1** and **2**, respectively); this is detrimental for an incoherent bridge-mediated mechanism and should favor a direct superexchange mechanism between the donor and the acceptor. For wires **3**−**5**, the more extended π-conjugation brings the LUMO of the bridge closer to that of the donor, thus opening the way for an active participation of the bridge in the charge-transfer process. The cyano substitution in compound **3′** lowers the energy of the LUMO level of the bridge below that of the corresponding electronic level in the donor; we can expect here the charge-transfer process to be initiated by a fast electron transfer from the donor to the bridge.

The calculated absorption spectrum of each DBA compound (Figure 4) shows three bands corresponding to the optical signature of tetracene (at 2.97 and 4.50 eV) and pyromellitimide (at 5.5 eV). The shape and position of these optical bands are rather insensitive to the nature and size of the bridge, thus reflecting a marked localization of the electronic excitations over the conjugated bridge, the donor, and the acceptor. The features calculated at 6.59, 3.90, 3.44, 3.20, 3.42, and 3.25 eV in compounds **1**, **2**, **3**, **3′**, **4**, and **5**, respectively, correspond to the lowest intense $\pi-\pi^*$ excitation of the phenylene-based segment. The wave function of the excited state leading to the optical feature at 2.97 eV has actually a small contribution arising from the bridge, which increases when going from **1** to **5** and is the largest for **3′**. The efficiency of the mixing between electronic excitations localized over the donor and the bridge can be intuitively understood on the basis of a two-level model involving the lowest optically allowed excited state of the two subunits. When the coupling between the two excitations is small with respect to their energy difference (which is always the case here), the amount of mixing between the two excited states is controlled by their relative energies:[48] the smaller the energy difference, the larger the mixing. That the largest interaction occurs for compound **3′** can be understood by the fact that the energy separation between the lowest bands with a dominant D* and B* character is the smallest there, as shown in Figure

(45) Mataga, N.; Nishimoto, K. *Z. Phys. Chem.* **1957**, *13*, 140.
(46) Newton, M. D. *Chem. Rev.* **1991**, *91*, 767.
(47) Shuai, Z.; Brédas, J. L. *Phys. Rev. B* **2000**, *62*, 15452.
(48) Ratner, M. A., Schatz, G. C., Eds. *Quantum Mechanics in Chemistry*; Prentice Hall: Englewood Cliffs, 1993.

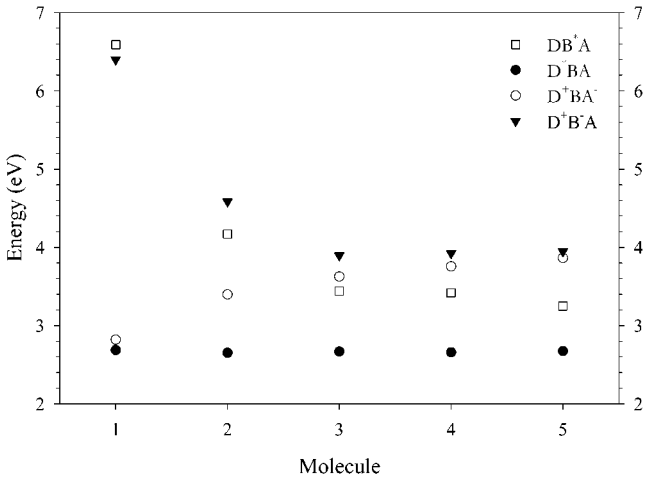

Figure 5. INDO/SCI transition energies from the ground state to excited states D*BA (●), DB*A (□), D^+BA^- (○), and D^+B^-A (▲). The relaxed D*BA geometry (Q_R) is considered in all cases.

4. Note that all the transition energies computed for the DBA systems are blue-shifted by about 0.4 eV with respect to the experimental measurements of Davis et al.[24] This can be attributed, at least partly, to the neglect of the solvent effects in the INDO/SCI calculations.

The excited states computed on the basis of the D*BA geometry (Q_R in Figure 2) can be classified according to their wave function characteristics. We find among them: (i) neutral excitations that are mostly localized on the donor (D*BA), the bridge (DB*A), or the acceptor (DBA*) part of the molecule; and (ii) charge-separated excitations, where the electron is transferred from the donor to the acceptor (D^+BA^-), the donor to the bridge (D^+B^-A), or the bridge to the acceptor (DB^+A^-). Such charge-transfer excited states can hardly be identified in the absorption spectra since the oscillator strengths associated to such transitions are usually very weak due to the confinement of the electron and hole wave functions over different parts of the molecule. As described above, the charge generation from the D*BA state can result from the following: (i) direct electron transfer from the donor to the acceptor (with the possible formation of superdonor and/or superacceptor units); or (ii) initial electron transfer from the donor to the bridge followed by a second transfer from the bridge to the acceptor. Another scenario is to involve first an energy transfer from the donor to the conjugated bridge (D*BA to DB*A) and next an electron transfer to the acceptor. However, the energy transfer process is expected to be relatively inefficient due to the limited spectral overlap between the lowest bridge absorption band (evolving from 6.59 eV in **1** to 2.75 eV in **5**) and the tetracene emission band (at 2.35 eV[49]). We will thus focus on the lowest D*BA, D^+BA^-, and D^+B^-A states to estimate the photoinduced charge-transfer rates in the molecular wires under study.

While the INDO/SCI gas-phase energy of the lowest D*BA excited state hardly depends on the length of the conjugated bridge, the lowest D^+BA^- excited state is gradually destabilized when the donor−acceptor separation increases (Figure 5). This mainly results from the reduction in Coulomb attraction between the positive and negative charges centered on the donor and acceptor groups when the bridge is elongated. In **1**, **2**, **3**, and **3′**, D^+BA^- is mainly described by an electronic transition from the HOMO (localized on the donor) to the LUMO (localized on the acceptor). Note that in **1**, an additional electronic transition from the HOMO-1 (delocalized over the donor and the bridge) to the LUMO contributes to the description of the D^+BA^- excited state and allows for some contribution of the bridge to the charge transfer.

(49) Madelung, O., Schulz, M., Weiss, H., Eds. *Landolt-Börnstein: Numerial Data and Functional Relationships in Science and Technology*; Springer-Verlag: Berlin, 1985; Vol. 17, p 186.

Table 1. ZDO (Zero Differential Overlap) Charge Distributions (in |e|) Computed at the INDO/SCI Level for the Charge-Transfer Excited States D^+BA^- and D^+B^-A in the Q_R Geometry

	D^+BA^-			D^+B^-A		
	D	B	A	D	B	A
1	+0.8	+0.2	−1.0	+0.6	−0.4	−0.2
2	+1.0	0.0	−1.0	+0.7	−0.6	−0.1
3	+1.0	0.0	−1.0	+0.5	−0.5	0.0
3′	+1.0	0.0	−1.0	+0.7	−0.7	0.0
4	+0.9	+0.1	−1.0	+0.5	−0.5	0.0
5	+0.6	+0.2	−0.8	+0.6	−0.6	0.0

In **4** and **5**, the highest occupied molecular orbital localized on the bridge is also involved in a charge-transfer excitation contributing to the description of the D^+BA^- excited state; this has to be related to the energy gap between the HOMO of the donor and that of the π-segment. In **2**, **3**, and **3′**, this gap is too large (0.77, 0.40, 0.86 eV, respectively) to allow for a significant contribution from charge-transfer excitations involving the HOMO of the bridge to the description of both the D*BA and D^+BA^- states; the energy offset is significantly reduced in **4** (0.32 eV) and **5** (0.21 eV) where such excitations contribute to some extent to the description of the lowest D*BA and D^+BA^- excitations (despite the large twist angles between the three parts of the molecule). These trends are also reflected in the INDO-SCI charge distribution in the D^+BA^- excited state, as calculated within the ZDO (zero differential overlap) approximation for the molecule in the Q_R geometry (see Table 1).

The charge transferred in the lowest D^+B^-A state is systematically smaller (though higher than 0.5 |e|) than that in the lowest D^+BA^- state; see Table 1. The absence of unit charge transfer between the donor and the bridge (which we used for practical reasons in our approach when calculating the reorganization terms and the free enthalpy of reaction) stems from the nature of the D^+B^-A excited states, which results from the mixing of two dominant types of configurations: (i) transitions from the donor to the conjugated bridge yielding the charge-transfer character; and (ii) transitions localized on the bridge (DB*A). The energy of the D^+B^-A state evolves in parallel to that of the DB*A state in the series due to the strong contribution of transitions localized on the bridge and the weak evolution of the effective charge-transfer distance. The partial charge transfer in the D^+B^-A state gives a finite probability of finding the electron on the bridge after excitation of the donor and is assumed to generate a fully relaxed charge-separated D^+B^-A state as an intermediate step in the complete transfer process.

B. Electronic Coupling Terms. The electronic coupling V_{RP} between the D*BA and D^+BA^- states decays with increasing separation between the donor and acceptor groups in compounds **1**, **2**, and **3** (Figure 6). This sharp evolution is representative of the superexchange mechanism observed in biological systems.[23] Strikingly, V_{RP} does not vanish in **3′**, **4**, and **5**, and actually increases when going from **3′** to longer oligomers, up to values

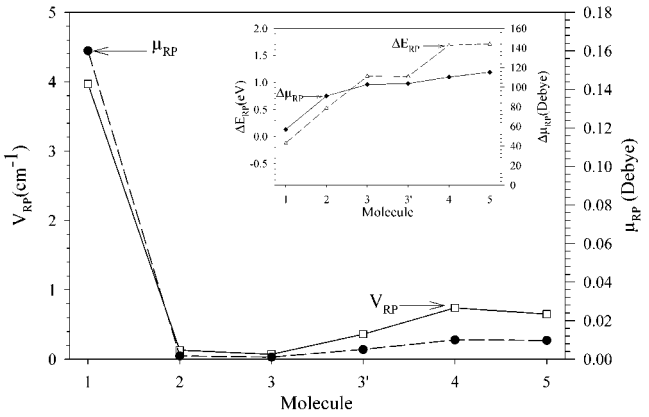

Figure 6. Electronic couplings, V_{RP} (□), and transition moments, μ_{RP} (●), for the D*BA/D$^+$BA$^-$ charge-transfer process. The energy offsets, ΔE_{RP} (△), and state dipole differences, $\Delta\mu_{RP}$ (◆), are shown in the inset.

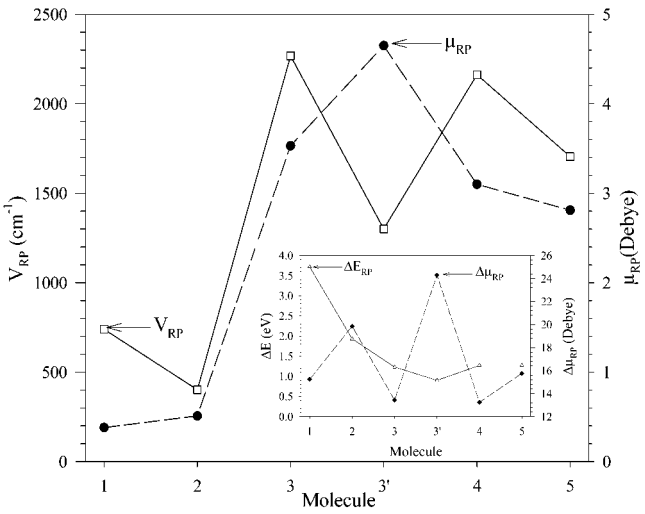

Figure 7. Electronic couplings, V_{RP} (□), and transition moments, μ_{RP} (●), for the D*BA/D$^+$B$^-$A charge-transfer process. The energy offset, ΔE_{RP} (△), and state dipole differences, $\Delta\mu_{RP}$ (◆), are shown in the inset.

on the order of 0.3−0.8 cm^{-1} (in comparison to ∼4 cm^{-1} in compound **1**). Analysis of the molecular parameters entering Mulliken−Hush's expression of V_{RP} (Figure 6) reveals that the transition dipole moment μ_{RP} between the excited states is the key factor determining the observed evolution. Its magnitude can be related to the overlap between the initial and final wave functions.

We first note that, except otherwise modified, the couplings have been computed here on the basis of the optimized values for the torsion angles between D/B and B/A units, that is, 70° and 32°, respectively. The decrease in V_{RP} when going from **1** to **3** results from a strong localization of the donor and acceptor electronic levels in compounds **2** and **3**, which strongly reduces the spatial overlap between the LUMO levels of the D and A units, and hence the transition dipole moment μ_{RP} between the D*BA and D$^+$BA$^-$ excited states, as the size of the bridge is elongated. The increase in μ_{RP} in **3′**, **4**, and **5** arises from the delocalization of the D unoccupied levels over the bridge, as discussed above.

To make sure that the computed μ_{RP} values for compounds **2**−**5** do not result from numerical artifacts, we have estimated the transition dipole moment between the D*BA and D$^+$BA$^-$ states for **2**, **3**, **3′**, **4**, and **5** when the central bridge is removed. In all cases, we find vanishingly small μ_{RP} values; note also that similar results are obtained when doubling the CI active space. We can thus conclude that in compounds **3′**, **4**, and **5**, the tetracene excited state gets a slight contribution from the bridge (weak "superdonor" effect) which enhances the electron-transfer rate. The increase along the series of the other two components appearing in the generalized Mulliken−Hush expression (eq 15), ΔE_{RP} and $\Delta\mu_{RP}$, is primarily governed by the progressive separation between the donor and the acceptor; the dipole moment of the D$^+$BA$^-$ state (and thus $\Delta\mu_{RP}$) is amplified with increasing donor−acceptor distance, and the energy of this state gets progressively destabilized due the reduction in the Coulomb attraction energy between the photogenerated charges (see Figure 6).

The electron transfer from D*BA to D$^+$B$^-$A is characterized by much larger electronic couplings than those calculated for the superexchange mechanism. V_{RP} displays strong variations when changing the length of the conjugated bridge (see Figure 7). In compounds **1** and **2**, V_{RP} is calculated to be on the order of 750 and 400 cm^{-1}, respectively, while it reaches values between 1300 and 2300 cm^{-1} in **3**, **3′**, **4**, and **5**. As is the case for the superexchange mechanism, μ_{RP} drives the evolution of the electronic coupling, except for **3′** where V_{RP} is 1000 cm^{-1} smaller than in **3**, although μ_{RP} is larger.

As pointed out previously, the D*BA excited states are mainly described by single-electron excitations localized on the donor (d → d*), which start mixing with the bridge b → b* transitions when the conjugated segment elongates; the D$^+$B$^-$A excited-state wave functions include charge-transfer d → b* excitations as well as some contributions from b → b* transitions. The actual transition dipole moment between the D*BA and D$^+$B$^-$A excited states is thus governed by the spatial overlap between the frontier unoccupied levels of the donor and the bridge (mainly the lowest unoccupied levels) as well as by shared configurations in the description of the two states. In compounds **1** and **2**, the energy offset between the frontier unoccupied levels of the bridge and the donor is larger than in molecules **3**−**5** (see Figure 3), which rationalizes the smaller transition dipole moment and electronic couplings calculated for these two molecules.

The increase in $\Delta\mu_{RP}$ when going from **1** to **2** originates from the interplay between the amount of charge transferred to the acceptor and the distance separating the donor from the acceptor. In compounds **3**, **3′**, **4**, and **5**, the evolution of $\Delta\mu_{RP}$ is driven by (i) the extent of the charge distribution over the bridge, which is enhanced upon cyano substitution and leads to a smaller electronic coupling for **3′**; and (ii) the amount of charge transferred to the bridge (Table 1). In contrast to the D$^+$BA$^-$ state, the energy of the D$^+$B$^-$A state is progressively stabilized when the size of the conjugated segment is elongated due to a progressive stabilization of the bridge unoccupied levels (while the average separation between the center of the positive and negative charge distributions evolves only weakly with chain length).

The charge transfer from the D$^+$B$^-$A state to the D$^+$BA$^-$ state is characterized by a much lower electronic coupling (decreasing from 37 to 1 cm^{-1} in going from **1** to **5**) than that computed for the electron transfer from the donor to the bridge (Figure 8). Note that these values have been obtained by considering that the system has sufficient time to relax after

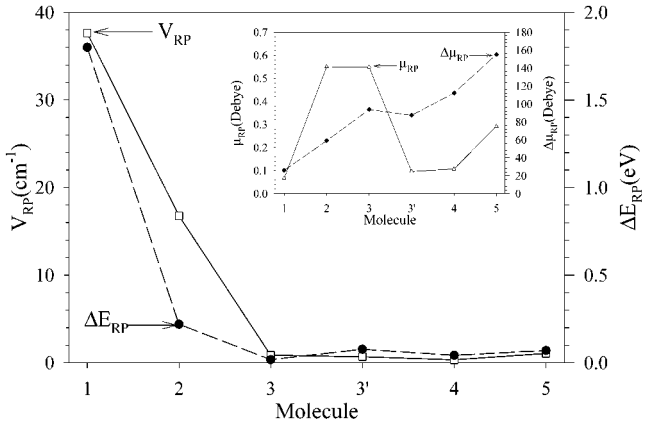

Figure 8. Electronic couplings, V_{RP} (□), and energy offsets, ΔE_{RP} (●), for the D^+B^-A/D^+BA^- charge-transfer process. The transition moments, μ_{RP} (△), and state dipole differences, $\Delta\mu_{RP}$ (◆), are shown in the inset.

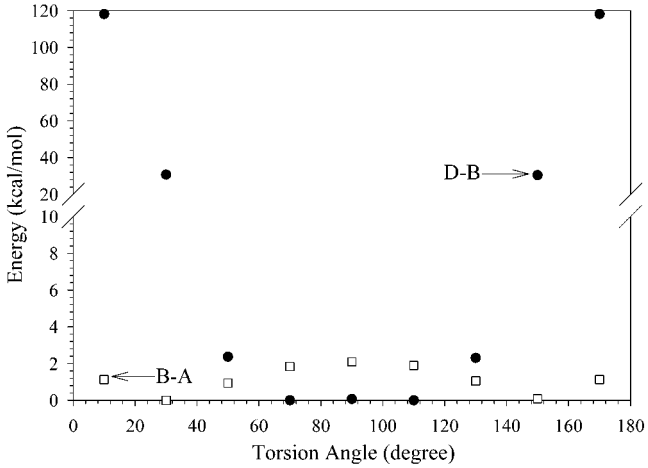

Figure 9. AM1 (rigid-rotor) ground-state potential energy curves for molecule **3**, with respect to the torsion angles between the donor and the bridge (●) and between the bridge and the acceptor (□).

the first transfer event and is thus in the relaxed geometry of the D^+B^-A state before the second transfer occurs; this assumption is justified by the rather slow transfer rates (1−4 ps^{-1}) measured experimentally[24] as compared to typical vibrational relaxation rates. Geometry relaxation in the intermediate state affects mainly the state energy, while the charge distribution remains nearly unaltered. In contrast to the previous cases, the evolution of ΔE_{RP} is here the key parameter controlling the magnitude of V_{RP}. The evolution of the energy difference between the two states along the series results from a compensation between (i) the destabilization of the D^+BA^- state linked to the reduction of the Coulomb attraction between the electron and the hole, and (ii) the stabilization of the D^+B^-A state discussed previously. The larger transition dipole moments calculated for molecules **2**, **3**, and **5** originate from a delocalization of high-energy unoccupied electronic levels describing the D^+B^-A state over the bridge and the acceptor units (i.e., a superacceptor effect); $\Delta\mu_{RP}$ is progressively amplified for increasing donor−acceptor separation.

The exact nature of the charge-transfer excited states is sensitive to the torsion angles in the donor/bridge and bridge/acceptor pairs. Because the potential energy surfaces associated to variations in torsion angles between the different units (determined on the basis of AM1 calculations in the rigid rotor approximation) are relatively flat around the equilibrium geometries (Figure 9), the molecules can adopt several conformations at room temperature,[31] which leads to significant variations in V_{RP}. To assess the influence of conformational fluctuations on the charge-transfer dynamics, we have evaluated the evolution of the electronic couplings computed for molecule **3** (similar trends are obtained for the other compounds) as a function of the torsion angles between the subunits. Note that in these calculations the bridge structure was kept frozen in its AM1-optimized conformation (not necessarily planar); the impact of rotational freedom along the bridge conjugated path on the temperature dependence of the electron-transfer rate has been explored in detail in ref 31. The evolution of the total energy of **3**, as calculated at the AM1 level, indicates that, at room temperature, the donor−bridge torsion angle, θ_1, can vary in the range 50°−130°, while the full range from 0° to 180° is accessible for the bridge−acceptor torsion angle, θ_2 (Figure 9).

The conformational fluctuations strongly influence the calculated electronic couplings; see Figure 10. These evolve with the values of the torsion angles over more than 1 order of magnitude for the D^*BA/D^+BA^- and D^+B^-A/D^+BA^- charge-transfer processes. The D^*BA/D^+BA^- coupling varies significantly as a function of the donor−bridge torsion angle and displays a quasi-symmetric distribution around $\theta_1 = 90°$ (the slight asymmetry reflects the high sensitivity of the coupling to the relative orientations of the three segments of the wire). As expected, V_{RP} is exalted when the angle between the donor and the bridge is reduced and is vanishingly small at 90°, where the two units are the most strongly decoupled. A smaller and somewhat chaotic dependence of V_{RP} is calculated with respect to θ_2, the bridge−acceptor torsion angle. Thus, it appears that hybridization between bridge and acceptor orbitals is not the key parameter for controlling the D^*BA/D^+BA^- electron-transfer process, at least for extended bridges. For the superexchange mechanism, the evolution of the electronic coupling as a function of the molecular geometry in **3** results essentially from the amount of mixing between the bridge and donor electronic levels.

The strength of the electronic coupling for the D^*BA/D^+B^-A transition varies with the donor/bridge torsion angle and (as expected) is hardly affected by the actual torsion between the bridge and acceptor units. The largest couplings are calculated for the smallest torsion angles (θ_1) between D and B. The increase in V_{RP} with decreasing θ_1 originates from a larger delocalization of the frontier molecular orbitals over the donor−bridge entity, which provides a better overlap between the empty molecular orbitals in the initial and final states, and hence boosts the corresponding transition dipole moment; these delocalization effects also lead to a reduction in the amount of charge transferred between the two units.

Finally, the evolution of the coupling term between the D^+B^-A and D^+BA^- states is driven by the changes in μ_{RP} and ΔE_{RP}, which result from a subtle interplay between charge distribution and electronic delocalization in the excited states. In this case, V_{RP} shows a more pronounced dependence on θ_2, while it is almost unaffected by θ_1. This is not surprising since the electronic coupling between D^+B^-A and D^+BA^- in molecule **3** was found to partly stem from a superacceptor effect (vide supra).

We note that the role of the solvent has not been considered when computing the various parameters entering the Mulliken−

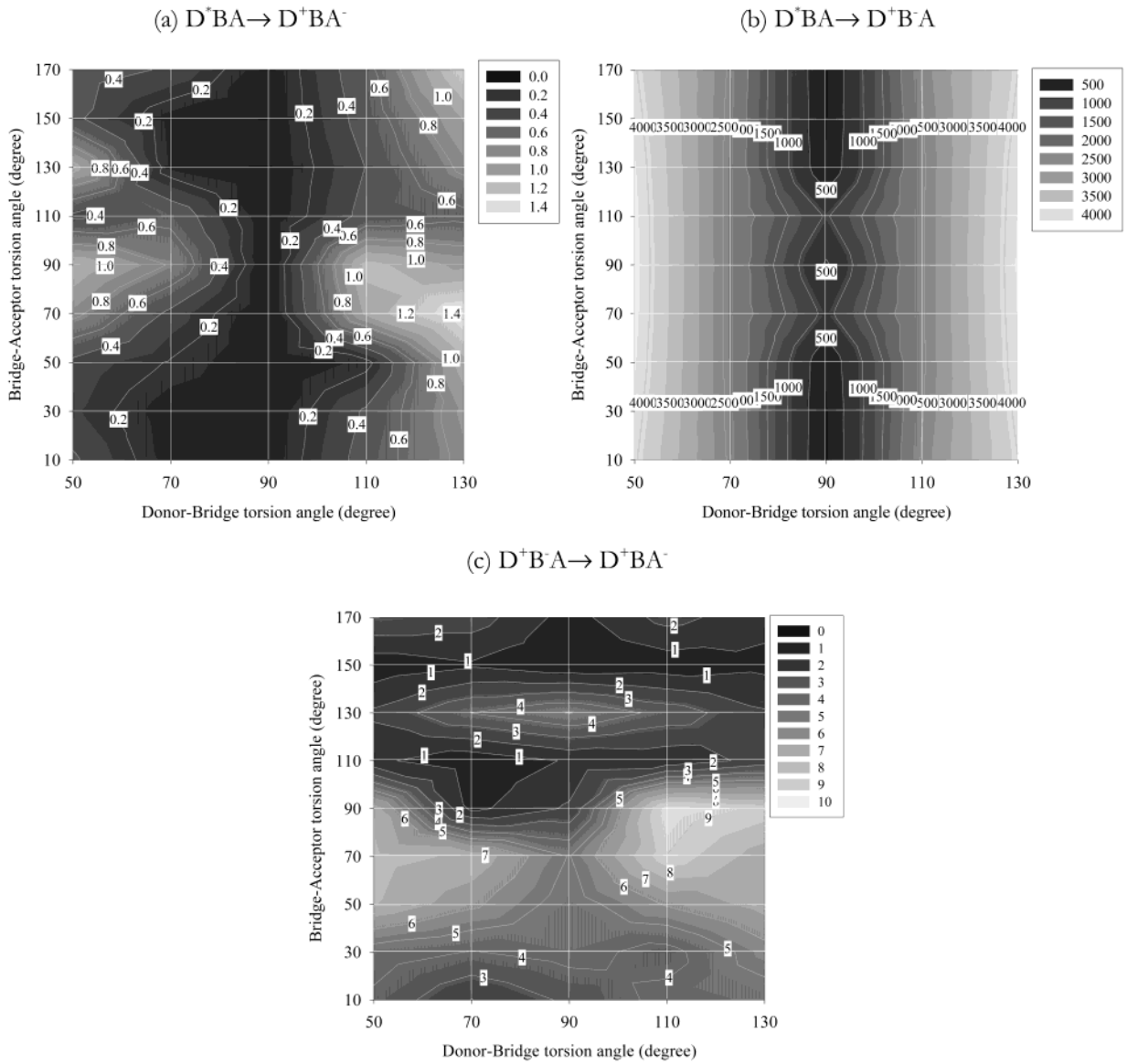

Figure 10. Evolution with the donor-bridge, θ_1, and bridge-acceptor, θ_2, torsions angles of the electronic coupling in molecule **3**, as computed for (a) the superexchange (D*BA/D$^+$BA$^-$) process; (b) the electron-transfer process from the donor to the bridge (D*BA/D$^+$B$^-$A); and (c) the transfer process from the bridge to the acceptor (D$^+$B$^-$A/D$^+$BA$^-$).

Hush expression used to estimate the electronic coupling between the initial and final states. In specific cases, the solvent has been shown to enhance the electronic coupling, for instance, in rigid DBA systems depending on their conformation[50] as well as in Zn/Zn$^+$ self-exchange reactions (an increase in V_{RP} by about 50% is predicted when considering neighboring water molecules).[51] In our case, the solvent effects are expected to stabilize the energy of the charge-transfer excited states, and hence to modify the ΔE_{RP} terms. Because the transition dipole moment between the two excited states is the main factor governing the evolution of the electronic coupling for the D*BA/D$^+$BA$^-$ and D*BA/D$^+$B$^-$A transitions, we do believe that the solvent effects will not alter the picture provided by the gas-phase calculations and will just lead to small modifications in the computed V_{RP} terms. Moreover, we do not expect the solvent effects to significantly amplify the weak coupling terms associated to the D$^+$B$^-$A/D$^+$BA$^-$ transition.

C. Reorganization Energies (λ) and Free Gibbs Energies ($\Delta G°$). As mentioned in the Theoretical Methodology section, we have evaluated the inner-sphere reorganization energies under the assumption that unit charge transfer occurs between the donator and acceptor units. Because the relaxation energy between the oxidized and excited geometries of the donor is relatively small, the main contribution to λ_i comes from the reduction of the acceptor units. For the bridge-mediated charge transfer, the internal reorganization energy typically ranges from 0.15 to 0.40 eV (except for **1**); see Table 2. The small λ_i value calculated for the D*BA → D$^+$B$^-$A transfer in **1** is due to the fact that the central benzene ring shows negligible geometric deformations upon charge injection. Elongation of the conjugated bridge in **2**, **3**, **3′**,**4**, and **5** is accompanied by an extension of the geometry deformations that consist in bond-length

(50) Cave, R. J.; Newton, M. D.; Kumar, K.; Zimmt, M. B. *J. Phys. Chem.* **1995**, *99*, 17501.
(51) Miller, N. E.; Wander, M. C.; Cave, R. J. *J. Phys. Chem.* **1999**, *103*, 1084.

Table 2. Internal (λ_i) and Solvent (λ_s) Reorganization Energies (in eV) for the Superexchange Mechanism (D^*BA/D^+BA^-) and the Two-Step Electron-Transfer Mechanism: Donor to Bridge (D^*BA/D^+B^-A) and Bridge to Acceptor (D^+B^-A/D^+BA^-) (See Text for Computational Details)

	D^*BA/D^+BA^-		D^*BA/D^+B^-A		D^+B^-A/D^+BA^-	
	λ_i	λ_s	λ_i	λ_s	λ_i	λ_s
1	0.15	0.59	0.04	0.37	0.21	0.44
2	0.15	0.77	0.25	0.46	0.42	0.60
3	0.15	0.86	0.15	0.61	0.31	0.65
3′	0.15	0.86	0.17	0.61	0.27	0.65
4	0.15	0.91	0.18	0.63	0.33	0.67
5	0.15	0.95	0.19	0.66	0.33	0.70

Table 3. Total Reorganization Energy ($\lambda = \lambda_i + \lambda_s$), Electronic Coupling ($V_{RP}$), and Free Gibbs Energy ($\Delta G°$) for the Direct and Indirect Electron-Transfer Processes[a]

	D^*BA/D^+BA^-				D^*BA/D^+B^-A			D^+B^-A/D^+BA^-		
	λ	V_{RP}	$\Delta G°$	$\Delta G°_{exp}$	λ	V_{RP}	$\Delta G°$	λ	V_{RP}	$\Delta G°$
1	0.74	4.0	−1.07	−0.84	0.41	739.0	0.98	0.65	37.6	−2.39
2	0.92	0.1	−1.00	−0.77	0.71	401.7	0.44	1.02	16.8	−1.74
3	1.01	0.1	−0.97	−0.74	0.76	2267.9	0.07	0.96	0.8	−1.28
3′	1.01	0.4	−0.97		0.78	1300.2	−0.52	0.92	0.7	−0.64
4	1.06	0.7	−0.95	−0.72	0.81	2162.6	−0.02	1.00	0.3	−1.10
5	1.10	0.6	−0.94	−0.70	0.85	1704.4	−0.03	1.03	1.1	−1.05

[a] The experimental ($\Delta G°_{exp}$) values are also indicated for the D^*BA/D^+BA^- process. All values are in eV, except V_{RP} is in cm^{-1}.

modifications typical of polaronic defects in doped conjugated oligomers.[39,52]

Although 2-methyltetrahydrofuran is a weak polar solvent, the outer contribution to the total reorganization energy is significant (actually much larger than λ_i) and ranges from 0.59 to 0.95 eV for the superexchange mechanism and from 0.37 to 0.66 eV [0.44 to 0.70 eV] for the first [second] step of the bridge-mediated process (Table 2). This λ_s value increases with the separation between the charges (l_{DA} in eq 9) in **1**, **2**, **3**, and **3′**, and saturates around a constant value for longer bridges (where the Coulomb attraction between the electron and the hole is strongly attenuated). It is worth stressing that the criterion of "weak interaction" limit required to use Marcus−Jortner−Levich's nonadiabatic formalism ($\lambda/2 \geq V_{RP} \geq 0$) is fulfilled for the two charge-transfer mechanisms in all the molecules investigated (see Table 3).

Analysis of the calculated free Gibbs energy variations ($\Delta G°$) shows (Table 3) the following: (i) The superexchange process is exoenergetic for all the wires. The computed values are in reasonable agreement with the experimental measurements of Davis et al.[23,24] (the mean deviation between experimental and theoretical results is ∼0.23 eV). (ii) The electron injection from the donor to the bridge is highly endoenergetic for **1** and **2**, and is expected to be thermally activated for **3**, **4**, and **5**. The addition of the cyano substituents on **3** significantly reduces $\Delta G°$ and leads to a bridge-mediated electron-transfer process in **3′** which is exoenergetic. (iii) The electron injection from the bridge to the acceptor is highly exoenergetic in all cases.

D. Charge-Transfer Rates (k_{RP}). Plugging all the calculated parameters into Marcus−Jortner−Levich's formula [eqs 2 and 4] allows us to evaluate the relative charge-transfer rates for the superexchange mechanism (with possible superdonor and/or superacceptor effects directly included in our calculations)

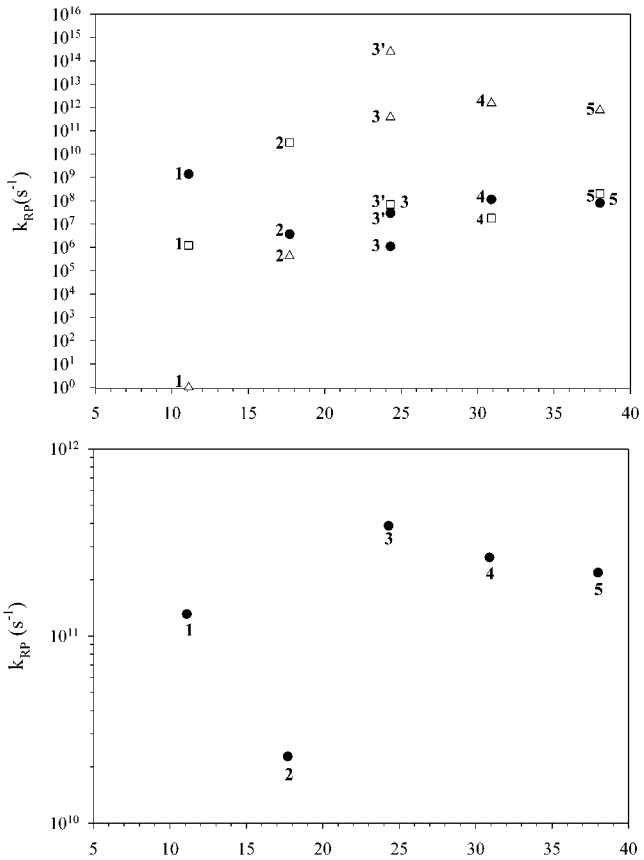

Figure 11. Top: Evolution of the electron-transfer rate with the distance separating the donor from the acceptor (in Å) in the case of the D^*BA/D^+BA^- (●), D^*BA/D^+B^-A (△), and D^+B^-A/D^+BA^- (□) charge-transfer processes. Bottom: Experimental charge-transfer rates, from ref 24.

and the two-step mechanism for the various compounds. As is generally assumed,[53,54] a single effective mode at 0.2 eV (corresponding to the C═C double bond vibration mode) has been considered to take into account the role of vibrations in assisting the transfer.

The comparison of k_{RP} for the two mechanisms (Figure 11) reveals that the relative rates vary considerably among the compounds. In **1** and **2**, superexchange is faster than the first step of the bridge-mediated process, implying that a direct tunneling of electrons occurs in these two wires; the decrease in k_{RP} when going from **1** to **2** is mostly driven by the reduction in V_{RP}. Despite the fact that the electronic coupling is much larger for the bridge-mediated process than for the superexchange mechanism, the former process is actually impeded by the high endothermic contribution calculated for **1** and **2**. In contrast, the first step of the indirect electron-transfer becomes the fastest process in **3**, **3′**, **4**, and **5** due to both the favorable thermodynamic conditions (small $\Delta G°$) and the large electronic couplings. The electron transfer from the donor to the bridge is 100 times faster in these compounds than the superexchange in **1** and **2**; strikingly, the rate of superexchange remains almost constant in **3**, **3′**, **4**, and **5** and thus deviates from the expected exponential decay law with respect to the donor−acceptor distance. These results demonstrate that superexchange can occur at large distances in situations where superdonor and/or

(52) Brédas, J. L.; Street, G. B. *Acc. Chem. Res.* **1985**, *18*, 309.
(53) Hubig, S. M.; Bockman, T. M.; Kochi, J. K. *J. Am. Chem. Soc.* **1996**, *118*, 3842.
(54) Closs, G. L.; Miller, J. R. *Science* **1988**, *240*, 440.

Table 4. Mean Values ($\langle k_{RP} \rangle$) and Variations ($[k_{RP}]$) (Determined on the Basis of the Standard Deviations:

$$[k_{RP}] = \langle k_{RP} \rangle \pm \sqrt{\frac{n\sum_n k_{RP}^2 - (\sum_n k_{RP})^2}{n(n-1)}}$$

Where n Is the Number of Conformations Considered) of the D*BA/D$^+$BA$^-$, D*BA/D$^+$B$^-$A, and D$^+$B$^-$A/D$^+$BA$^-$ Electron Transfers Computed for the Room-Temperature Accessible Conformations of Molecules **2** and **3**[a]

	D*BA/D$^+$BA$^-$			D*BA/D$^+$B$^-$A			D$^+$B$^-$A/D$^+$BA$^-$		
	$\langle k_{RP} \rangle$	$[k_{RP}]$	k_{RP}	$\langle k_{RP} \rangle$	$[k_{RP}]$	k_{RP}	$\langle k_{RP} \rangle$	$[k_{RP}]$	k_{RP}
2	3.00×10^9	4.78×10^8—5.43×10^9	3.68×10^6	3.98×10^6	5.33×10^5—7.42×10^6	4.32×10^5	2.15×10^{10}	5.32×10^7—4.29×10^{10}	3.18×10^{10}
3	9.13×10^7	1.59×10^6—1.81×10^8	1.10×10^6	8.86×10^{11}	1.52×10^{11}—1.62×10^{12}	3.78×10^{11}	2.10×10^9	1.26×10^8—4.08×10^9	7.09×10^7

[a] The ground-state values (donor-bridge and bridge-acceptor angles of 72° and 30°, respectively) are indicated as a reference (k_{RP}).

superacceptor units arise from strong mixing between the donor [acceptor] and bridge electronic structure.

Because the bridge-mediated electron transfer occurs in two steps, a complete description of the process also requires one to estimate the electron-transfer rate from the bridge to the acceptor. Although $\Delta G°$ favors this second step, its efficiency is significantly reduced by very weak electronic coupling terms between the D$^+$B$^-$A/D$^+$BA$^-$ states, calculated to be on the order of 1 cm^{-1} in **3**, **3′**,**4**, and **5**. All together, our calculations suggest that the electron transfer from the bridge to the acceptor represents the limiting step of the "bridge-mediated" process and competes with the superexchange mechanism. In this scenario, the bridge-mediated transfer might be distinguished through the detection of the optical signature of the polaron created on the bridge in the intermediate state by means of transient absorption measurements; we emphasize that the recent data collected by Davis et al.[24] do not provide clear experimental evidence for such a reduction of the bridge (possibly because the bridge population is too small to be observed in the transient absorption).

The impact of conformational disorder on k_{RP} has been probed for molecules **2** and **3** by computing for each process the average value of V^2_{RP} and its standard deviation (Table 4). We expect that these results are representative of the trends prevailing for the other compounds under study. When considering the ensemble of accessible conformations at room temperature, it appears that (i) the superexchange rate calculated for the equilibrium geometry is underestimated with respect to the average value (by up to 2 orders of magnitude for **2**); (ii) the electron-transfer rate from the donor to the bridge is less affected by the actual conformation adopted by the molecule (with variations up to 1 order of magnitude); and (iii) the electron-transfer rate from the bridge to the acceptor varies also significantly among the conformers and fluctuates by nearly 2 orders of magnitude in **2** and **3**. Note that the values obtained at the equilibrium geometry provide the upper and lower limits for molecules **2** and **3**, respectively. Switching from the equilibrium geometries to the conformations accessible at room temperature is thus expected to lead on average to (i) an increase of the D*BA → D$^+$BA$^-$ tunneling rate in short molecules, and (ii) electron hopping from the bridge to the acceptor in extended structures.

The various approximations inherent to our theoretical approach do not allow us to provide a full quantitative description of the electron-transfer phenomena in the molecules under consideration. However, an excellent qualitative agreement is observed between experiment and theory in terms of the distance dependence of the mechanism and dynamics of the electron transfer (Figure 11). In particular, we find that in extended structures (**3**−**5**), a mechanism involving transient population of the phenylenevinylene wire significantly contributes to the charge-transfer mechanism as a consequence of significant interaction between the donor and bridge electronic structures. This can translate into a transfer rate faster than that of the superexchange mechanism. The rate drop with increasing the distance is steeper for **1** and **2** than for **3**, **4**, and **5**, as seen experimentally. We attribute the deviations observed between the theoretical and experimental values mostly to (i) the large uncertainty concerning the actual conformational space spanned by the molecules (particularly torsional aspects[31]); (ii) the error on the values of the different parameters involved in Marcus−Jortner−Levich's expression of the transfer rate combined to the high sensitivity of the exponential function; and (iii) a breakdown of the Condon approximation due to the dependence of the electron-transfer rates on torsional motions.[31]

IV. Conclusions

We have developed a theoretical approach based on semiempirical techniques to evaluate the main parameters entering into the nonadiabatic vibronic theory of Marcus, Jortner, and Levich, to describe photoinduced electron-transfer rates in DBA molecules. Our quantum-chemical analysis provides a good insight into the factors determining the efficiency of short versus long-range charge-transfer mechanisms.

In the compounds under study, electron transfer results from a competition between a direct process and a "bridge-mediated" process, whose efficiency depends on the length and nature of the conjugated bridge. Superexchange electron transfer is the fastest process in the smallest molecules of the series (**1**, **2**) and is favored by a large exoenergetic contribution compensating the weak electronic coupling between the initial and final states. In contrast, electron transfer involving either a two-step (injection) mechanism or (to a lesser extent) superdonor/superacceptor effects appears to be the dominant process in extended wires (**3**, **4**, **5**). The results are fully consistent with the experimental observations and with expectations based on system bath

analyses[55−58] which suggest coherent (superexchange) decay at short distances and large gaps, hopping (injection) for longer bridges.

We have also shown that conformational disorder can strongly modulate the electronic coupling terms and hence lead to significant fluctuations in the electron-transfer rates. We expect that the approach described in this work can be useful to better understand the mechanisms of photoinduced charge transfer in other systems of great interest, such as DNA strands, photosynthetic centers, or blends used in organic solar cells.

(55) Pollard, W. T.; Felts, A. K.; Friesner, R. A. *Adv. Chem. Phys.* **1996**, *93*, 77.
(56) Skourtis, S. S.; Mukamel, S. I. *J. Chem. Phys.* **1995**, *197*, 367.
(57) Davis, W. B.; Wasielewski, M. R.; Ratner, M. A.; Mujica, V.; Nitzan, A. *J. Phys. Chem. A* **1997**, *101*, 6158.
(58) Segal, D.; Nitzan, A.; Davis, W. B.; Wasielewski, M. R.; Ratner, M. A. *J. Phys. Chem. B* **2000**, *104*, 2790.

Acknowledgment. The work at Arizona is supported by the National Science Foundation (CHE-0078819), the Office of Naval Research, and the IBM Shared University Research Program. The work in Mons is supported by the Belgian Federal Government "InterUniversity Attraction Pole in Supramolecular Chemistry and Catalysis (PAI 4/11)" and the Belgian National Fund for Scientific Research (FNRS-FRFC). D.B. and J.C. are FNRS Research Fellows. M.R. thanks the Chemistry Divisions of ONR and NSF for support.

JA017150+